CHAPTER 4

CHARACTERIZATION OF THE PRODUCED ACTIVATED CARBONS

4.1 Introduction

The studied properties of activated carbon were surface area, mesopore volume, total pore volume, pore size, pore size distribution, surface chemistry, surface morphology and elemental composition. The five adsorbents were characterized using proximate analysis and FTIR but better activated carbon were characterized using elemental analysis, Scanning electron micrographs (SEM) and (Brunauer–Emmett–Teller) BET test analysis due to limiting budget in this research. Therefore, the objectives of this chapter was the physio-chemical characterization of the prepared activated carbon from rice husk, coconut coir, corn cobs, neem bark, and *Moringa oleifera* bark.

4.2 Materials

The prepared activated carbon of rice husk, coconut coir, corn cobs, neem bark, and *Moringa oleifera* bark were used which were discussed in Chapter 3.

4.3 Methods

4.3.1 Proximate Analysis of the Activated carbon

The values of moisture content, ash content and volatile matter of rice husk were determined according to the American Society for Testing and Materials, ASTM E1756-01, ASTM E1755-01 and ASTM E872-82, respectively (ASTM, 2006 and ASTM, 2007). The proximate analysis of the different type of activated carbon was done using the following procedure.

4.3.1.1 Determination of Moisture Content

2 g of activated carbon sample (rice husk) was weighted and then put in a container. It was spread nicely in the container. It was then heated in an oven at a temperature of 105˚C for 3 hr. The container was not covered during the heating process. After heating the container was detached and put in a desiccator. After cooling the dried sample was weighted.

$$(4.1)\quad \text{Moisture content (\% MC)} = \frac{(mf - mt)\ x\ 100}{(mi - mt)}$$

m_i = initial mass of container and biomass, and

m_f = final mass of container and biomass after drying at 105˚C

m_t = tare mass of dried container

Same procedure of moisture content was also followed for others activated carbon of coconut coir, corn cobs, neem bark and *Moringa oleifera* bark.

4.3.1.2 Determination of Volatile Matter Content

A known quantity (2 g) of activated carbon sample of rice husk was put in a cylindrical crucible closed with a lid. It was then heated to 950˚C for exactly 7 minutes using a muffle furnace. The crucible was put in a desiccator and measured. Volatile matter on dry basis.

Calculate the weight loss percent as follows:

$$(4.2)\qquad \text{Weight loss, \%} = \frac{(wi - wf)\ x\ 100}{(wi - wc)} = \text{A}$$

where: w_c = weight of crucible and cover, g

w_i = initial weight, g and w_f = final weight, g

Calculate the volatile matter percent in the analysis samples as follows:

(4.3) Volatile Matter in analysis sample, (% VM) = *A* - *B*

where: *A* = weight loss %, and

B = moisture, %, as determined using Method E1756-01.

Same procedure of volatile matter content was also followed for others activated carbon of coconut coir, corn cobs, neem bark and *Moringa oleifera* bark.

4.3.1.3 Determination of Ash Content

2 g of activated carbon sample of rice husk was put in a container. It was heated in a muffle furnace to 550˚c for 24 hrs. During this heating process the container was left open. After the required heating, the container was put in a desiccator and then the ash was weighted.

(4.4) Ash content (% A) = $\frac{(ma-mc)\ x\ 100}{(ms-mc)}$

% ash = mass percent of ash, based on 105°C oven-dried mass of the sample

m_c= tare mass of empty container, g

m_s= initial mass of 105°C dried sample and container, g

m_a=mass of ash and container, g

Same procedure of ash content was also followed for others activated carbon of coconut coir, corn cobs, neem bark and *Moringa oleifera* bark.

4.3.1.3 Fixed Carbon

(4.5) Fixed carbon FC = 100 – (% moisture content+ % volatile matter + % ash content)

4.3.2 Ultimate Analysis of the Activated Carbon

About 100 mg of samples was put on a double-sided electrically conducting carbon adhesive tape on SEM holder into Energy Dispersive X-Ray (FESEM-EDX) analyser. The elemental analysis used in the EDX was performed using (ZEISS SUPRA 40VP SEM) for the activated carbon of coconut coir due to having a limited budget. The EDX detector was equipped with an ultra-thin light-element window detecting elements with an atomic number > 4. The Energy Dispersive X-Ray analyser was used to detect the elements like carbon, sulphur, oxygen, nitrogen, silica, sodium and chlorine etc. in the sample. The sample was set in triplicate. Three blanks were involved in each analytical batch.

4.3.2 Surface Morphology

The surface morphology of the activated carbon was determined by Scanning Electron Microscope (SEM). It is also used to identify the pore structure, surface structure, and pore arrangement. The coating is a must for a non-conductive specimen (Fei, 2005). The coating was applied to raise the constancy of the beam. It also improves the image quality. The sample was coated with a 1 to 4 nm layer of Palladium in all directions. The coated sample was mounted onto the sample chamber with a sample holder. The instrument function settings were adjusted to compliment the analysis. The image was obtained by using an imaging procedure. Here the high voltage was ramped. The appeared image was focused and adjusted. It was modified to capture the high-resolution image (Pathan et al., 2010).

4.3.3 Surface Chemistry

Fourier Transform Infrared Spectroscopy was carried out to study the surface chemistry of the prepared activated carbons. It was proved by identifying the functional groups presented on the outer surface on the adsorbents. Various infrared light wavelengths were used to measure functional groups of five activated carbons. It was recorded using a suitable method (Higgins & Seelebinder, 2011). Prior analysis, firstly the background spectrum was collected. Then approximately, 0.05 g of sample was placed onto the crystal plate. The sample was put into the FTIR device. It was placed by turning down the knob until a 'click' sound. Then the sample was evaluated by spectrum and the created spectrum was saved for data analysis.

4.3.4 Experimental Setup for Furnace

The process of pyrolysis, carbonization, and activation of the precursor were conducted in a stainless-steel vertical furnace (Linn Elektro Therm, Germany). The furnace consisted of a fixed bed reactor, a vertical tubular electric furnace, a temperature controller, flow meters and a ventilation exhaust. The size of the vertical reactor is 100 cm length and 6.9 cm width of 310-grade stainless steel. The reactor was situated at a central place in the vertical tubular furnace. The system was involved with a temperature controller to control and monitor the temperature. The furnace can tolerate a maximum tolerant temperature of 1200 °C. The smoke discharged from the reactor was condensed in a water condenser through condenser tubing. The experimental setup for the preparation of the activated carbon is two parts discussed below: gas metering section to control the gas flow rate and temperature controller. The gas stream was delivered to the back side of the vertical furnace. It is attached to the reactor from the lower end of the tubular furnace. The Teflon tubing linked by stainless steel fittings was assembled as the connecting pipe for the system. Nitrogen (N_2) gas was supplied to the system at constant pressure. It was adjusted using pressure regulators. Here the flow rate was determined by gas flow meters.

4.3.5 Carbonization

About 100 g of the precursor was taken and placed into a furnace equipped with stainless steel vertical tubular reactor. Nitrogen gas was applied as the purging gas through the furnace, to prevent oxidation in the system. The flow rate of nitrogen gas was held at 1.5 mL/min. The heating rate was set constant at 10 °C/min. The temperature was increased from room temperature to 280 °C for corn cobs and neem bark and held for 5 hours. After the five-hours holding time, the temperature was decreased to 30 °C to collect the produced char. The rice husk, coconut coir and *Moringa oleifera* bark were carbonized at 700 ºC for a one hour. The char was taken in a desiccator. The char was then stored in an air-tight container like a polypropylene bottle for further treatment (Ahmad et al., 2011). Calculation of the char yield is as in equation 4.5:

$$Yield\ (\%) = \frac{Wc\ x\ 100}{Wi} \tag{4.6}$$

Where w_c is the mass of char (g) after carbonization process and w_i is the initial mass of corn cobs before carbonization.

4.3.6 Chemical Impregnation

The chars produced were impregnated with different chemicals at various impregnation ratios (IR) as shown in Table 4.1. The samples (100 g) were then chemically activated using 500 mL zinc chloride (w/v 10% $ZnCl_2$) and sulfuric acid (0.5M H_2SO_4) with ratio of 1:5 for 6 hours for *Moringa oleifera* bark (Salmi Abdullah et al., 2017). Rice husk was impregnated with zinc chloride ($ZnCl_2$) solution with a ratio of (1:2 ratio) for 16 hours (Shahmoradi et al., 2015). Coconut coir was soaked with (2%) sodium bi-carbonate ($NaHCO_3$) for 18 hours (Khan & Choudhuri et al., 2011). Corn cobs were soaked with zinc chloride (0.1M ratio 1:1) for 6 hours (Okafor et al., 2015). Neem bark was impregnated using zinc chloride (0.1M) and phosphoric acid (v/v 10% H_3PO_4) in two separate beakers as well as produced paste with a mixer for 3 hours (Kenneth et al., 2015). Then, the beaker with the impregnated sample was placed inside

an oven for 12 hours at temperature 110 °C for dehydrating purpose, leaving only excess chemicals from the sample. Each produced char was impregnated with different chemicals using three ratios like (1:1, 1:2, 1:5) and only the best impregnated ratio shown in Table 4.1.

The impregnation ratio was calculated as in equation 4.6:

$$IR = \frac{Wchar\ x\ 100}{Wchemical} \quad (4.7)$$

where $W_{chemicals}$ is the amount (g) or mL of chemicals and W_{char} is the dry weight (g) of char.

Table 4.1 The impregnation ratio (IR) using varieties chemical and char

Impregnated Ratio (IR)	Char (g)	Chemicals (g) or mL
1:2	Rice husk	$ZnCl_2$
1:5	Coconut coir	$NaHCO_3 + H_2SO_4$
1:1	Corn cobs	$ZnCl_2 + H_3PO_4$
1:5	Neem bark	$ZnCl_2 + H_3PO_4$
1:5	*Moringa oleifera*	$ZnCl_2 + H_2SO_4$

4.3.7 Pyrolysis for Activation

The varieties of chemicals impregnated chars were placed inside the furnace reactor for activation. It was conducted under the nitrogen flow of 150 cm^3/min. The temperature was increased from ambient temperature (25 °C) to desired activation temperature (600 °C, 700 °C and 800 °C). Here it was the heating rate of 10 °C/min. When the desired activation temperature was touched and held for one hour. The activated carbons were cooled to room temperature under nitrogen flow (Ahmad et al., 2011). All processes were conducted three times. Table 4.2 shows the activation

temperature applied for the activated carbon which was the best adsorption capacity for rice husk, coconut coir, and *Moringa oleifera* bark at 700 °C and corn cobs and neem bark at 800 °C during one hour.

Table 4.2 The activation temperature applied for 1 hour of each natural material

Activated Carbon	1st Temperature	2nd Temperature	3rd Temperature
Rice husk	600 °C	700 °C	800 °C
Coconut coir	600 °C	700 °C	800 °C
Corn cobs	600 °C	700 °C	800 °C
Neem bark	600 °C	700 °C	800 °C
***Moringa oleifera* bark**	600 °C	700 °C	800 °C

4.3.8 Washing

The produced adsorbents were cleaned with distilled water to remove the remaining $ZnCl_2$ and other chemicals like free acid and base. This process was continued until the pH of the washing solutions reached 6-7. The pH was measured using a pH meter. Here, the washing process was conducted by filter paper. Later it was then kept in an oven at 110 °C for 12 hours. After drying the activated carbons were stored in air-tight containers like polypropylene bottles for further characterization studies (Ahmad et al., 2011).

4.3.9 Surface Area and Porosity Measurement

The surface chemistry of produced adsorbents was conducted using the adsorption isotherms of nitrogen. It involved surface area, pore volume and pore size distribution of the prepared adsorbents. The surface area and porosity analyzer are run by measuring the quantity of gas adsorbed onto a solid surface. Here the static volumetric method is applied to measure the amount of gas absorbed. A quartz sample tube was used to hold

the analyzed sample. A cleaned quartz sample tube was weighed together with a frit seal using an analytical balance. That weight was documented. Approximately 1.0 gram of the fine sample was placed into the tube. It was weighed together with the frit seal and the weight was also noted. Then the samples were degassed from ambient temperature to 300 °C until the evacuation was completed at 950 mm Hg. After the degassing procedure was completed, the sample was kept in the analysis system for cooling in liquid nitrogen. A 21-points analysis was measured at -196.15 °C to obtain adsorption isotherm. Through admitting successive known volumes of nitrogen in and out of the sample and measuring the equilibrium pressure (Micromeritics, 2006). A relative pressure of between 10^{-5} and 0.995 of N_2 gas was used to obtain the N_2 adsorption isotherm. The Estimate of surface area and pore volume were performed by the software. It was calculated from the N_2 adsorption isotherms using the Brunauer-Emmett-Teller (BET), Langmuir and Barrett, Joyner, and Halenda (BJH) equations (Ahmad et al., 2012). In the meantime, the micropore volume has been measured by applying the Horvath–Kawazoe (HK) method (Örkün et al., 2012).

4.4 Results and Discussion

4.4.1 Characterization of the activated carbon

4.4.1.1 Proximate Analysis

Table 4.3 shows the proximate analysis between five precursors: rice husk, coconut coir, corn cobs, neem bark, and *Moringa Oleifera* bark. The comparisons were made to study the differences between the five precursors. The differences were studied in the (1) moisture content, (2) volatile content, (3) ash content and (4) the fixed carbon content. The percentage of moisture content in *Moringa oleifera* bark, corn cobs, neem bark, coconut coir, and rice husk were 1.3 %, 2.3 %, 4.6 %, 5.81 %, 4.5 % respectively. Besides, the percentage of volatile content in coconut coir, rice husk, neem bark, corn cobs, and *Moringa oleifera* bark were 15.5 %, 12.4 %, 10.21 %, 14.65 % and 14.40 % respectively. However, the percentage of ash content rice husk, neem bark, coconut coir, *Moringa oleifera* bark, and corn cobs were 7.25 %, 2.5 %, 1.4 %, 4.38 %, and 1.20 % respectively. The percentage fixed carbon of corn cobs (83.79 %) was significantly

higher and neem bark, *Moringa oleifera* bark, coconut coir, and rice husk were 75.16 %, 79.9 %, 82.8 %, and 75.95 % respectively. The ash content is a determination of the total amount of minerals in the sample. Char with a large proportion of mineral matter results in higher ash yields on an air dried basis (Saini et al., 2015). The pH of the soil could have effected the uptake of minerals and availability of nutrients to the natural trees. If acidity is increased, various nutrients and minerals could be unavailable. Some minerals can lead due to present excessively (Van Vliet et al., 2015).

Table 4.3 Proximate analysis of all adsorbents

Parameter	Rice husk	Coconut coir	Corn cobs	Neem bark	*Moringa oleifera* bark
Ash content (%)	7.25	2.5	1.4	4.38	1.20
Moisture content,(%)	1.3	2.3	4.6	5.81	4.5
Volatile content,(%)	15.5	12.4	10.21	14.65	14.40
Fixed carbon,(%)	75.95	82.8	83.79	75.16	79.9

4.4.1.2 Ultimate Analysis

The surface chemical composition was determined by using a Field Emission Scanning Electron Microscopy with Energy dispersive X-ray (FESEM-EDX) spectroscopy. The spectrum obtained was shown in Figure 4.1 and the percentage was summarized in Table 4.4. The percentage of carbon (C), sulphur (S), oxygen (O), chlorine (Cl), sodium (Na) were 76.1 %, 11.4 %, 10.8 %, 1 %, 0.8 %, respectively. The presence of carbon and oxygen were supported by FTIR results that showed the presence of carboxyl and hydroxyl groups. The presence of sodium appears in the spectrum indicating that the sodium compound was strongly bound with carbon and oxygen. Besides that the high percentage of carbon shows the nature of coconut coir that mainly is good for producing activated carbon. EDX analysis results are shown in Figure 4.1, where results are presented in the mass percentage of the sample. Coconut

coir was basically an organic structure with large amounts of carbon and oxygen. Some other elements were found too such as Sodium (Na), Silicon (Si), and Chlorine (Cl). The biochar sample showed a huge amount of carbon, oxygen and some amounts of Na, and Cl were also found.

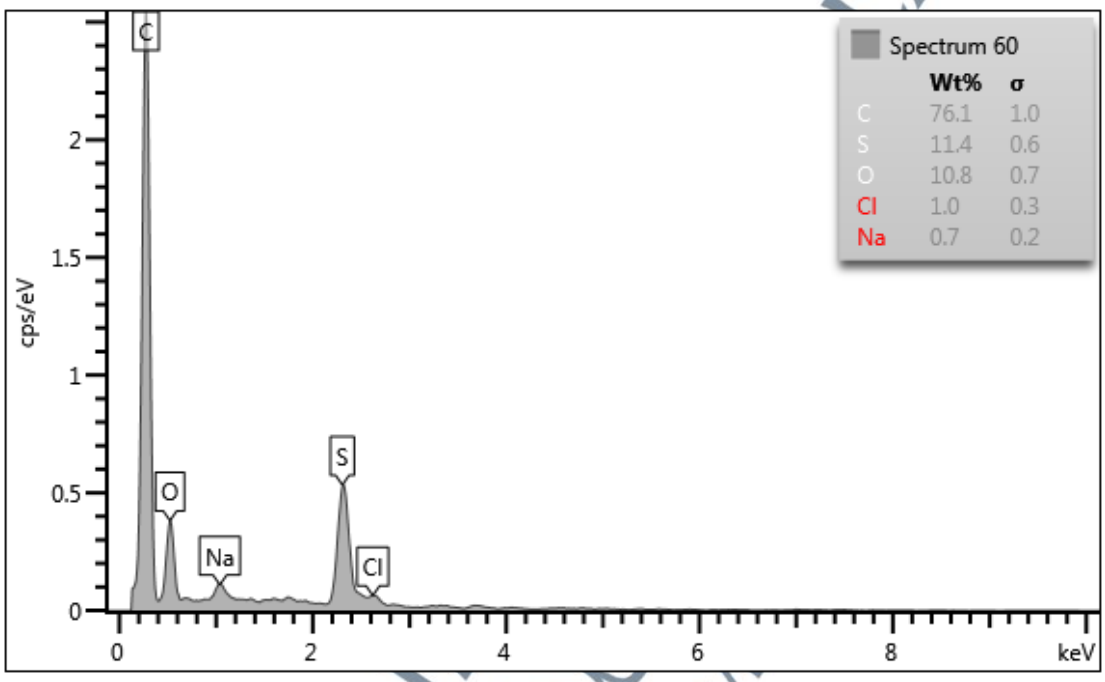

Figure 4.1 EDX analysis of the coconut husk and its derived char at 700°C.

Table 4.4 Weight percentage for the elements in coconut coir

Element	Weight percentage (%)
Carbon (C)	76.1
Sulphur (S)	11.4
Oxygen (O)	10.8
Chlorine (Cl)	1
Sodium (Na)	0.7

4.4.1.3 Surface Area and Porosity

Table 4.5 shows the surface area and porosity of the two best prepared activated carbon due to having a limited budget in this research. The BET surface areas were

detected to be relatively high. The BET surface area of *Moringa oleifera* bark was as high as 439.23 m^2/g than rice husk (271.85) when pyrolysis at 700 °C. It was micropore 396.93 m^2/g for *Moringa oleifera* bark. The total pore volumes measured were higher (0.153-0.189 cm^3/g). *Moringa oleifera* bark carbon was the best activated carbon among others due to impregnation with $ZnCl_2$ and H_2SO_4 in a specific activating agent to char ratio (5:1).

Table 4.5 Surface area and pore characteristics of the prepared activated carbons

Activated carbon	Pore Size Å	Micropore volume (cm^3/g)	Total pore volume (cm^3/g)	BET Surface Area (m^2/g)	Micropore Surface Area (m^2/g)
***Moringa oleifera* bark**	17.23	0.1537	0.1892	439.23	396.93
Rice husk	17.91	0.0941	0.1217	271.85	239.36

On the other hand, according to (Njoku & Hameed, 2011), the BET surface area was measured at 1,273 m^2/g from corn cob and 1,218 m^2/g from olive stones (Yakout & Sharaf El-Deen, 2016). The activated carbon was prepared using the chemical activation method stones (Yakout & Sharaf El-Deen, 2016). Alias et al., (2017) had studied the effectiveness of K_2CO_3 in producing the activated carbon with a higher number in surface areas and total pore volumes. They suggested that the improvement of the porous structure of adsorbents by K_2CO_3 activation is associated with gasification reaction, where K_2CO_3 accelerated the gasification process. During the heat treatment, the reduction of the potassium and the micro structural changes took place (Kamali & Fray, 2013). Biomass such as *Moringa oleifera* bark and other agricultural by-products formed of cellulose, lignin, and hemicellulose (natural polymer). During carbonization at high temperatures, the polymeric structures decompose. It releases most of the non-carbon elements, mostly hydrogen, oxygen, and nitrogen. It also releases minerals in the form of liquid (called tars) and gasses. The carbons which are left behind formed a

rigid carbon skeleton (Prahas et al., 2008). In cellulosic materials, the carbonization temperature was found to be a crucial factor in developing a highly porous carbon structure.

According to (Fałtynowicz et al., 2015), thermal decomposition started at 50 – 200 °C where it is associated with moisture release. Then, between 225 - 375 °C was where the most intensive decomposition of organic matter happened. The celluloses and hemicelluloses underwent decomposition and discharged the volatile contents. When the temperature improves, the decomposition rate decreases. Here, its minimum weight loss occurred due to the formation of char structural units which were more resistant to thermal decomposition. However, decomposition of higher thermal stability compounds took place, such as lignin. A total weight loss of approximately 75 % was recorded when the temperature reaches 700 °C. By referring to Table 4.5, a relatively similar phenomenon can be observed during this study. At temperature 700 °C and impregnated with char and $ZnCl_2$ at the ratio of 1:2 for rice husk (RH), the BET surface area was only developed at 271.85 m^2/g indicating the lesser formation of pores. This value (239.36 m^2/g) was calculated as microporous surface area. The median pore width was 8.64 nm (700 °C).

However, methods of activated carbon both rice husk and *Moringa oleifera* bark were same but when chemically activating agent H_2SO_4 was mixed with $ZnCl_2$ for *Moringa oleifera* bark (MOB), the surface area was increased to 439.23 m^2/g. The microporous surface areas were also increased to 396.93 m^2/g. The micropore volume of *Moringa oleifera* bark was 0.154 cm^3/g and pore diameter was 17.23 Å resulting in a highly microporous activated carbon. $ZnCl_2$ and H_2SO_4 play an important role in porosity development at different stages. When $ZnCl_2$ was introduced to the precursor during the impregnation process, the partial structure of *Moringa oleifera* bark was destroyed. $ZnCl_2$ altered the carbonization behaviour of *Moringa oleifera* bark, converted the contained minerals into soluble salts and established skeletal pore structure at the pre-carbonization period. Then, $ZnCl_2$ developed micropores abundantly and reduced the formation of graphitized carbon during the activation phase. It showed the impact of $ZnCl_2$ and H_2SO_4 in the development of new pores and the improvement of microporous structures in the carbon.

Figure 4.2 shows a plotted graph for the pore size distributions of *Moringa oleifera* bark and rice husk activated carbon due to have limiting budget, based on these data. As can be seen from this plot, singular sharp peaks were detected in the range of 20 to 40 Angstrom (Å) (or 2 to 4 nm).

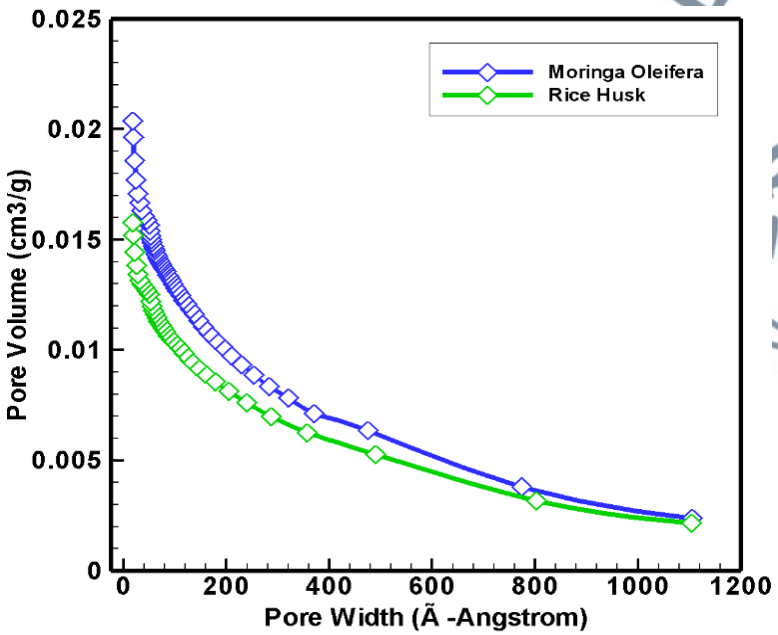

Figure 4.2 Pore size distribution of rice husk and *Moringa oleifera* bark

About 75 % of the pores had their diameter within the mesopores range (pore diameter range of 10–200 Å) for *Moringa oleifera* bark and (10 -180 Å) for rice husk. Hence, the activated carbon is mesoporous material. This suggests the prepared activated carbon would be very absorptive to wastewater. In inert condition, carbonization could yield a mesopore carbon of a very narrow pore size distribution. Carbon with narrow pore size distributions is stable in a structure that could increase practical parameters such as BET surface area and V_0 total micropore volume (Łukaszewicz & Zieliński, 2011).

4.4.1.4 Surface Morphology

Surface chemistry is a very important part of activated carbon for analysis. Figure 4.3 (a) and (b) shows the SEM micrographs of the *Moringa oleifera* bark char due to limiting budget of this research under 1000x and 30000x magnification for before adsorption and Figure 4.3 (c) and (d) are the micrographs of the activated carbon under 1000x and 30000x magnifications for after adsorption. Those micrographs presented the morphological changes of the carbon materials during carbonization and activation processes. After carbonization was performed under inert conditions. Several irregular holes were advanced on the surfaces of the chars. It can be observed in Figure 4.3 (a) and (b). This was due to the sudden burst of thermal expansion during pyrolysis. Pore enlargement in the char was essential. It would raise the surface area and pore volume of the activated carbon after the activation process (Ahmad & Alrozi, 2010).

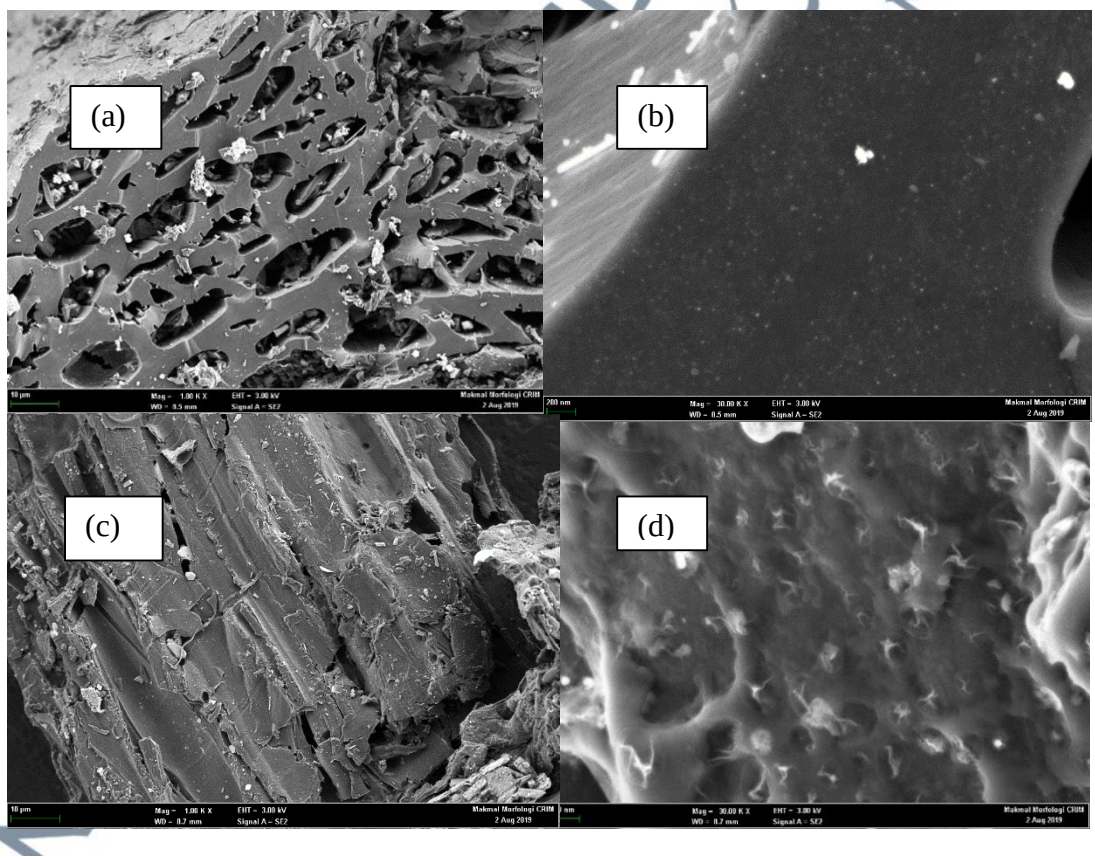

Figure 4.3 SEM micrograph of *Moringa Oleifera* bark (a)-mag.-1000x and (b)-mag.-30,000x before and (c)-mag.-1000x and (d)-mag.-30,000x) after activation.

In Figure 4.3 (a), (b) for *Moringa oleifera* bark more heterogeneous and irregular shape pore structures were observed. More pores were advanced and were closed to each other. $ZnCl_2$ with sulphuric acid-impregnated sample shows a better porous structure development. At this point, the porous structure has been formed. Here, exterior pores serve as the main channels. It connects to the inner pores of the carbon. However, the structure has been partly destroyed. When the surface was eroded during the activation process. Here a similar observation was obtained by (Guo & Deng, 2013). The introduction of $ZnCl_2$ enlarged the difference between the morphology on the surface of the char and of the activated carbon. The reactions between $ZnCl_2$ and carbon took place due to the diffusion effect. The heat was carried into the molecules. It can create more pores in the activated carbon (Tan et al., 2008). (Okman et al., 2014) observed spongy-like structures with many small cavities in the grape seed based activated carbon which was impregnated with K_2CO_3. It can be observed in Figure 4.3 (c) and (d) the presence of small white particles of various sizes attached to the surface of the activated carbon. The white particles were believed to be the residues of zinc salt (from $ZnCl_2$). Even a similar finding was observed by (Mopoung, 2008) while making the activated carbon from banana peel. This indicates that the traces of zinc salts residues are present in the carbon matrix even though a serious washing procedure with the combination of HCl and distilled water was applied.

4.4.1.5 Surface Functional Groups

Fourier-Transform Infrared Spectroscopic analysis played a vital role in analysing functional groups on the surface of produced activated carbon. Figure 4.4-4.8 exhibits the similarities in the pattern of the FTIR spectrum for the five natural husk and bark-based activated carbon. Table 4.10 lists the wave numbers of the FTIR spectrum detected in the carbon. It can be observed that in the infrared spectrum for the prepared activated carbon, peaks were detected at 663, 665, 742, and 664 cm^{-1} C-H (Ar) for rice husk, coconut coir, corn cobs, and *Moringa oleifera* bark but the peak of C-H stretching was not detected for neem bark. There are some common functional groups in most of

the given activated carbon such as OH stretching, CH stretching, C=C stretching and C-O stretching.

The broad and intense peaks at 3350, 3382, 3376, and 3372 cm^{-1} were determined from rice husk, coconut coir, corn cobs, and *Moringa oleifera* bark, respectively for OH stretching. It was attributed to hydrogen bonding. The peaks at 1542, 1556, 1600, 1632 and 1432 cm^{-1} were determined due to C=C stretching of aromatic or olefinic bands for rice husk, coconut coir, corn cobs, neem bark, and *Moringa oleifera* bark, respectively. Oxygen functional group (C=O) was not detected in the prepared activated carbon. The intense peaks at 1076, 1095, 1000, 1026, and1123 cm^{-1} were obtained due to C-O stretching of alcohol or carboxylic acid for rice husk, coconut coir, corn cobs, neem bark and *Moringa oleifera* bark, respectively. The adsorption capacity of neem bark was not well for metal adsorption due to not having available the intense peak for C-H stretching of aromatic ring and O-H stretching. After being loaded with a different metal of activated carbon, the peaks for C-O, C=C, and O-H had shifted slightly. This can be occurred due to bonds with metal and functional groups. This type of shifting relied on the concentration of metals that were loaded in activated carbon according to literature (Çelekli & Bozkurt, 2011 and Azouaou et al., 2010). The surface quality of the adsorbent is determined by the Fourier-Transform Infrared Spectroscopic analysis as shown in Figures 4.4-4.8.

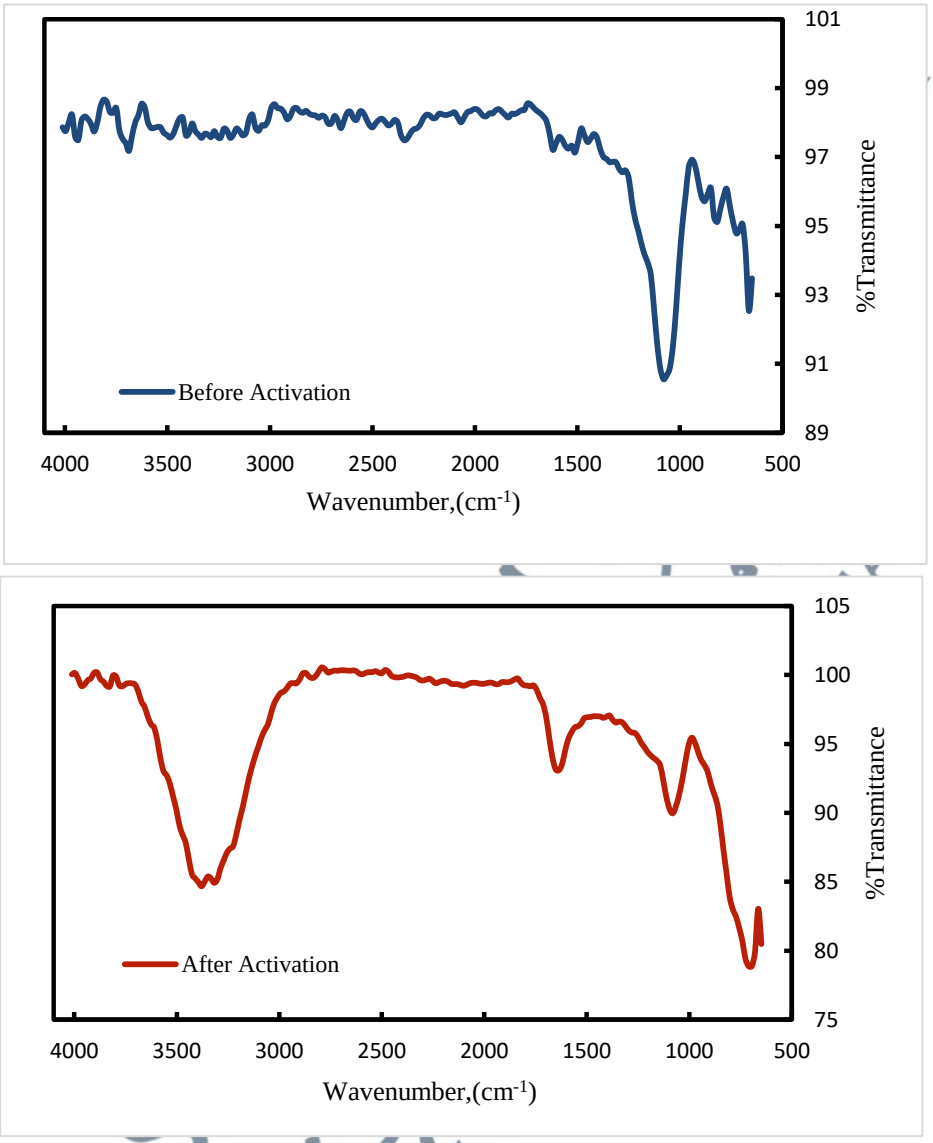

Figure 4.4 FTIR spectra for before and after activation on rice husk

Table 4.6 Comparison of FTIR band positions of raw rice husk before and after metal ions activation in wave number (cm^{-1}).

Assignment	Before activation	After activation
O-H stretching (3600-3200)	3350	3380
C-H stretching (<900 for Ar)	663	694
C=C Stretching (Aromatic) (1620-1400)	1544	1642
C-O stretching (1300-1080)	1076	1062

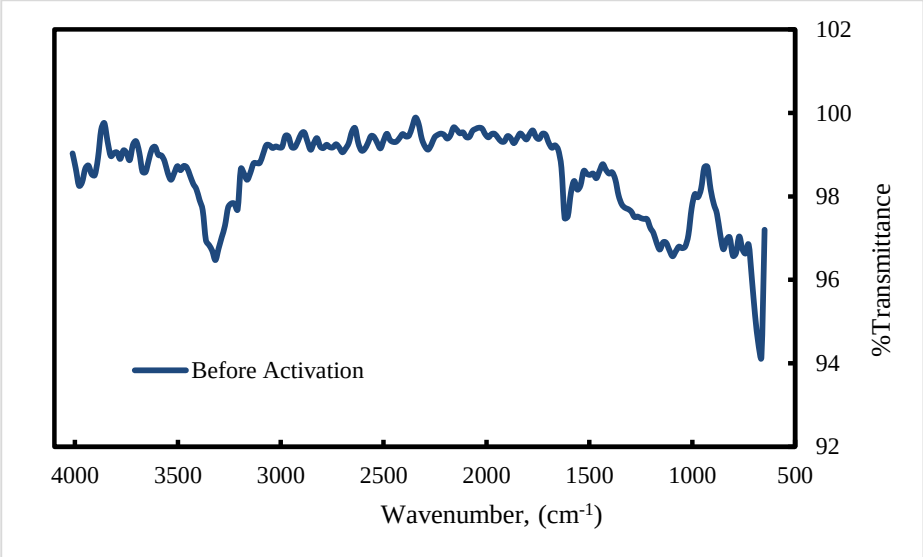

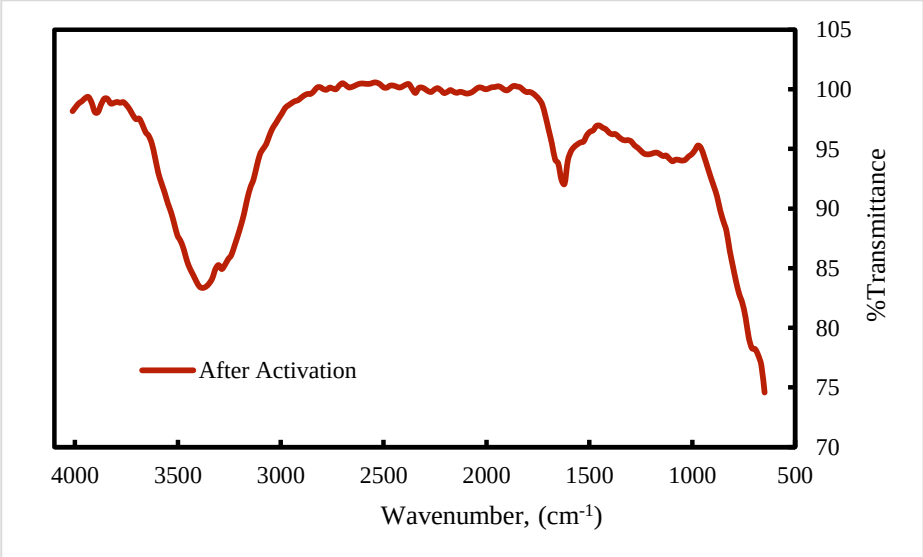

Figure 4.5 FTIR spectra before and after activation on coconut coir

Table 4.7 Comparison of FTIR band positions of raw coconut coir before and after activation in wave number (cm^{-1})

Assignment	Before activation	After activation
O-H stretching (3600-3200)	3382	3379
C-H stretching (<900 for Ar)	665	648
C=C Stretching (Aromatic) (1620-1400)	1556	1638
C-O stretching (1300-1080)	1095	1050

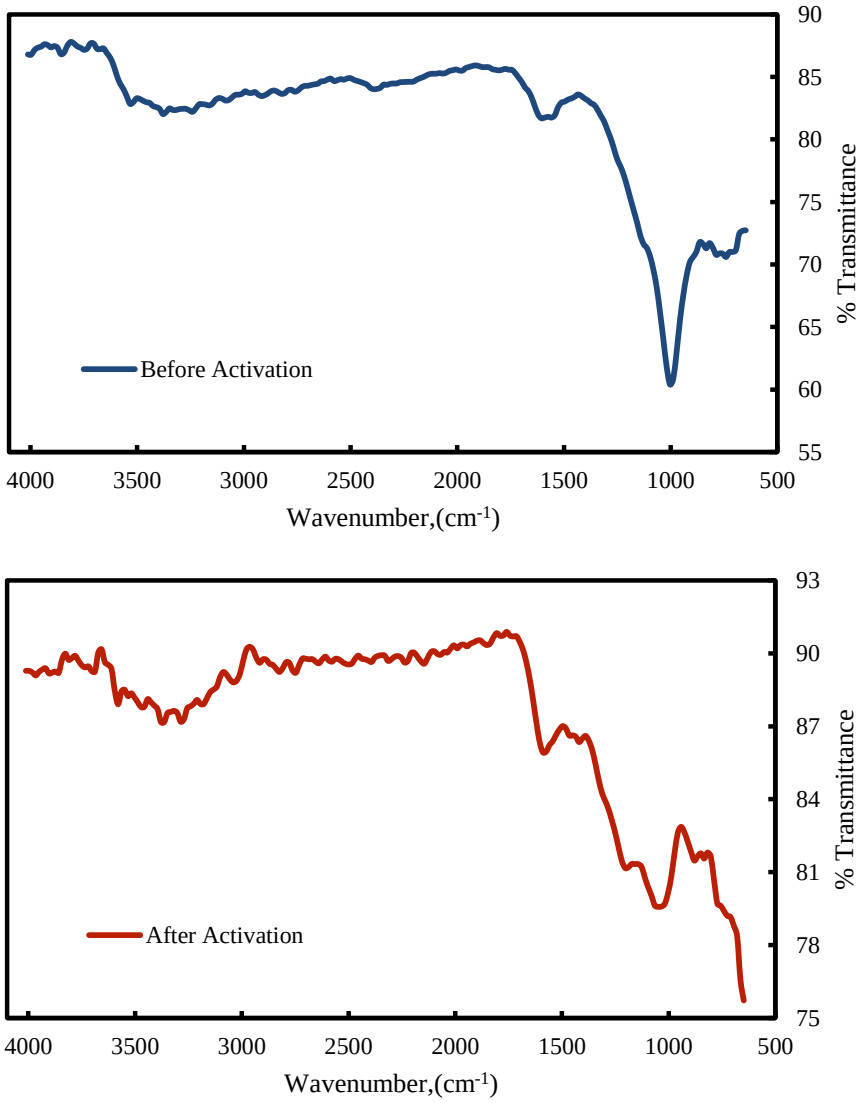

Figure 4.6 FTIR spectra before and after activation on corn cobs

Table 4.8 Comparison of FTIR band positions of raw corn cobs before and after activation in wave number (cm^{-1})

Assignment	Before activation	After activation
O-H stretching (3600-3200)	3376	3371
C-H stretching (<900 fo Ar)	-	-
C=C stretching (Aromatic) (1620-1400)	1600	1583
C-O stretching (1300-1080)	1000	1050

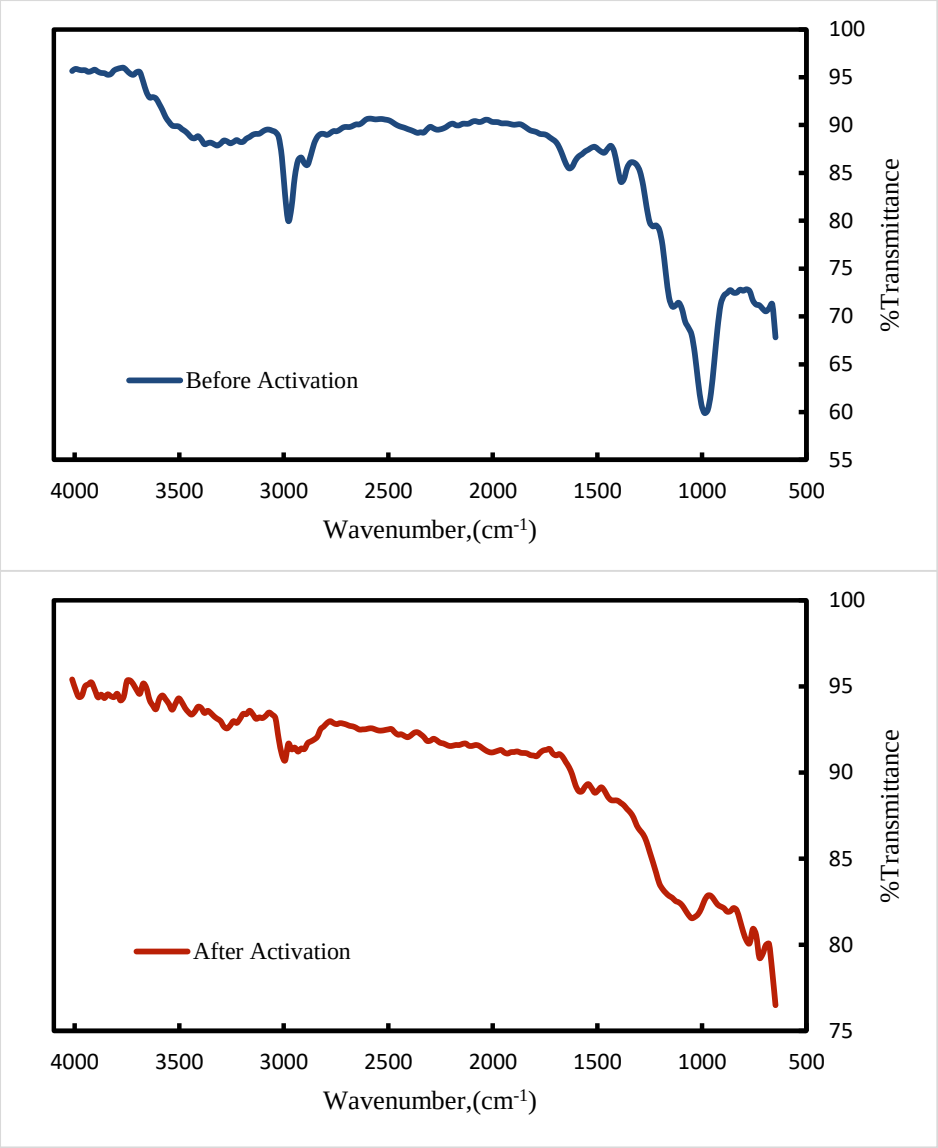

Figure 4.7 FTIR spectra before and after activation on neem bark

Table 4.9 Comparison of FTIR band positions of raw neem bark before and after activation in wave number (cm^{-1})

Assignment	Before activation	After activation
C=C stretching (>3000 for Aliphatic)	3002	3005
C-H stretching (<900 for Ar)	-	-
C=C Stretching (Aromatic) (1620-1400)	1632	1581
C-O stretching (1300-1080)	1000	1020

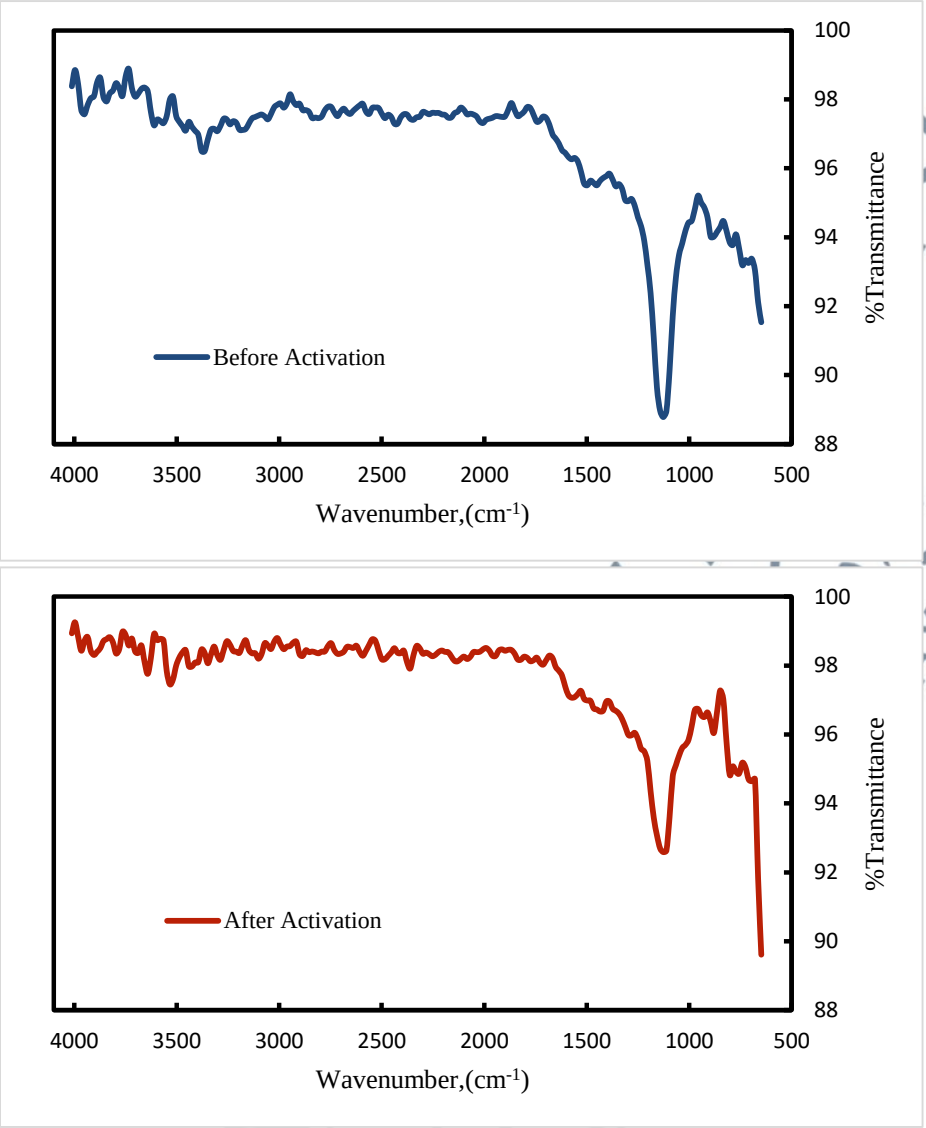

Figure 4.8 FTIR spectra before and after activation on *Moringa oliefera* bark

Table 4.10 Comparison of FTIR band positions of raw *Moringa oleifera* bark before and after activation in wave number (cm^{-1})

Assignment	Before activation	After activation
O-H stretching (3600-3200)	3371	3500
C-H stretching (<900 for Ar)	664	648
C=C stretching (Aromatic) (1620-1400)	1501	1432
C-O stretching (1300-1080)	1126	1123

Table 4.11 Infrared assignment of functional groups on the prepared activated carbon surface (Adapted from Ahmad et. al., 2013)

Characteristics	**Wave number Length**	**Activated Carbon**				
Aliphatic Hydrocarbon	Range	Rice Husk	Coconut Coir	Corn Cobs	Neem Husk	*Moringa Oleifera*
C-H	3100-2850	2914	No	No	No	3183
C=C	>3000	3010	3164	No	3002	No
C=-C	2260-2100	2260	2250	No	No	No
Aromatic HC						
C-H (out of Plane)	<900	663	665	742		664
C=C	1620-1400	1544	1556	1600	1632	1501
Combined bands	1900-1700	No	No	No	No	No
Oxygen functional groups						
C-O	1300-1080	1076	1095	1000		1126
O-H	3600-3200	3350	3382	3376	3374	3371

4.4.1.6 Adsorption Isotherm of the two best Activated Carbon

Due to limiting budget and its characteristics, the activated carbon prepared at 700 °C with impregnated by different chemically activating agents like $ZnCl_2$ for rice husk and $ZnCl_2$ with H_2SO_4 for *Moringa oleifera* bark were selected to undergone the activation process.

Figure 4.9 demonstrates the adsorption isotherms of *Moringa oleifera* bark and rice husk. The different shapes of the adsorption isotherm are a reflection of the different pore size distribution in adsorbent samples. It can be suggested that the isotherms of rice husk and *Moringa oleifera* bark resembled a combination of types II and I with prominent hysteresis loops of type H_4, which occur in the region of 0.02 to 0.08 P/Po. This displays the higher degree of mesoporosity contained in both carbons (Mak et. al., 2009).

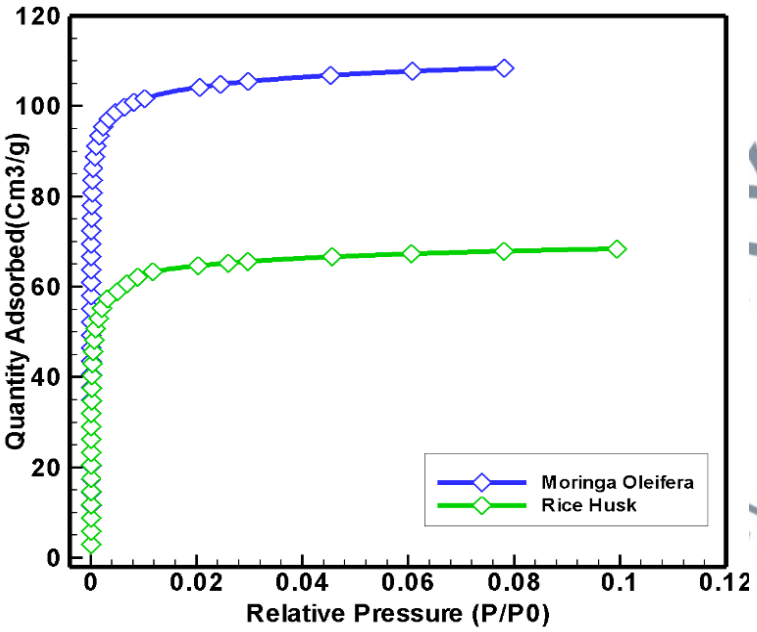

Figure 4.9 Adsorption isotherm of rice husk and *Moringa oleifera* bark

Both carbons showed a less steep Type I isotherm with a sharp "knee" form at the low relative pressure and a regular increase in nitrogen gas (N_2) adsorb at the higher pressure. The regular increase in N_2 adsorb occurred beyond P/Po > 0.02, thus presenting the heterogeneous microporosity and growth of small size mesoporosity (Nakagawa et al., 2007). Acid treatment increased the adsorbed amount of nitrogen for *Moringa oleifera* bark in the region of 0 to 0.1 P/Po. Both isotherms presented with a steep adsorption at very low relative pressures (P/Po = 0 to 0.02) characteristic of microporous structures (Nakagawa et al., 2007). The hysteresis loop type H_4 considered the presence of mesopores particles. *Moringa oleifera* bark exposed the higher adsorption and rice husk exhibited the lowest adsorption of the series in the low-pressure region. Acid treatment improved the quantity adsorbed at low relative pressures. *Moringa oleifera* bark was adsorbed with almost more N_2 than rice husk, which indicates a higher surface area. The sloped-up plateau started at P/Po > 0.02. The increase in N_2 bind at the other pressures indicated the rise of micropore diameter and development of mesoporosity (Nakagawa et al., 2007).

4.5 Conclusion

The activated carbon of rice husk, coconut coir, corn cobs, neem bark, and *Moringa oleifera* bark were characterized by proximate analysis and FTIR but only best activated carbon were also characterized using SEM, BET and ultimate analysis due to having a limited budget. This research indicated that the use of $ZnCl_2$ with H_2SO_4 as well activating agent along with the pyrolysis under inert condition. It played a vital role in producing natural husk or bark into well-advanced porosity activated carbon. It produced mostly microporous carbon with an average pore diameter of 17.23 Å nm. However, the prepared activated carbon contained deposited $ZnCl_2$ and inorganic constituents on the surface. Several cleaning processes were applied to remove some of these deposits to develop porosity. The HCl treatment on the prepared activated carbon managed to reduce the remaining minerals. For this reason, it was developed as a highly porous carbon structure. Activated carbons from *Moringa oleifera* bark and rice husk were shown the best adsorbents among the others produced activated carbons in this study.